Chemical Engineering Science 116 (2014) 1–8

Contents lists available at ScienceDirect

Chemical Engineering Science

journal homepage: www.elsevier.com/locate/ces

# Scalability of mass transfer in liquid–liquid flow

A. Woitalka [a], S. Kuhn [a,b,*], K.F. Jensen [a,**]

[a] Department of Chemical Engineering, Massachusetts Institute of Technology, Cambridge, MA, USA
[b] Department of Chemical Engineering, University College London, London, UK

## HIGHLIGHTS

- The scalability of mass transfer in liquid–liquid flow is addressed.
- The obtained results highlight the dependence of mass transfer on the two-phase flow patterns.
- On the milli-scale fluid–structure interactions are driving the interfacial mass transfer.
- Reactor designs promoting fluid–structure interaction ensure straightforward scalability from the micro- to the milli-scale.

## ARTICLE INFO

*Article history:*
Received 7 February 2014
Received in revised form
16 April 2014
Accepted 25 April 2014
Available online 8 May 2014

*Keywords:*
Liquid–liquid flow
Interfacial mass transfer
Scale-up
Micro-reactors
Milli-reactors

## ABSTRACT

We address liquid–liquid mass transfer between immiscible liquids using the system 1-butanol and water, with succinic acid as the mass transfer component. Using this system we evaluate the influence of two-phase flow transitions from Taylor flow to stratified flow and further to dispersed flow at elevated flow rates. In addition, we address the scale-up behavior of mass transfer coefficients and the extraction efficiency by using reactors on the micro- and the milli-scale. Flow imaging enables us to identify the different flow regimes and to connect them to the trends observed in mass transfer, and the obtained results highlight the dependence of mass transfer on flow patterns. Furthermore, the results show that on the milli-scale fluid–structure interactions are driving the phase dispersion and interfacial mass transfer, and such a reactor design ensures straightforward scalability from the micro- to the milli-scale.



## 1. Introduction

Microreaction technology is widely used in research and development for rapid experimentation and shortening product development cycles, as it provides several advantages over conventional, and mostly batch, reaction systems (Ehrfeld et al., 2000). As an example, using an automated flow microreactor system allows for the fast determination of the kinetic information of a specific reaction, which significantly reduces development times (Zaborenko et al., 2011). This is possible since the decrease in length scale leads to an increased surface-to-volume ratio on the micro-scale, which is beneficial to obtain enhanced mass and heat transfer coefficients. Early studies showed the potential of using microreactors for chemical synthesis in small-scale flows (Jensen, 2001), and Hartman et al. (2010) report the development of more complex microchemical systems to enable multi-step processes.

Enabling such multi-step processes on the micro-scale is an important contribution to process intensification as converting traditional batch processes to continuous flow can lead to an increase in production (Anderson, 2012). The paper resulting from the ACS GCI Pharmaceutical Roundtable which is co-authored by several major pharmaceutical and fine chemistry companies also identified the need for further research efforts in process intensification, and the demand for novel concepts for continuous reaction systems (Jimenez-Gonzalez et al., 2011). Furthermore, continuous manufacturing allows us to access novel process windows (Hessel and Wang, 2011; Hessel and Noël, 2012a,b) which can be exploited further to intensify the involved chemical processes.

Despite all these advantages of microchemical devices, one of their major challenges is that in terms of economical production they lack sufficient throughput to meet industrial needs. Increased production is difficult to achieve by numbering up (scale-out) individual devices due to the associated challenges in providing a stable fluid distribution, and thus the loss in residence time distribution control. Consequently, scale-up by increasing the characteristic dimensions of the flow reactors to achieve enlarged internal volume is still a necessary step to bring flow chemistry to

* Corresponding author at: Department of Chemical Engineering, University College London, London, UK.
** Corresponding author.
*E-mail addresses:* simon.kuhn@ucl.ac.uk (S. Kuhn), kfjensen@mit.edu (K.F. Jensen).

http://dx.doi.org/10.1016/j.ces.2014.04.036

production scale. Therefore it is desirable to develop continuous mini reaction systems in the millimeter scale, which combine the advantages of micro-reactors, i.e. faster mixing, enhanced heat and mass transfer, and a narrow residence time distribution, with the throughput of conventional batch reactor systems.

An alternative to pure scale-up is represented by a combined scale-up and scale-out approach. Such a potential scale-up/scale-out route is given by the Advanced Flow Reactors made by Corning, which are designed in a periodic heart shape structure to improve mixing, interfacial mass transfer, and wall heat transfer (Lavric, 2008; Zhang et al., 2011). These individual milli-scale reactor units then provide the possibility for scale-out to adjust the throughput. For a single phase reaction, these systems have been successfully employed to scale-up the reaction conditions developed using a standard microreactor (McMullen et al., 2010). The two-phase flow behavior of the Corning Advanced-Flow Reactor (AFR) and the quantification of gas–liquid mass transfer were addressed in Nieves-Remacha et al. (2012, 2013).

However, many of the relevant chemical transformations involve multiphase flow, either gas–liquid, immiscible liquids, or solid–liquid. Thus, to successfully design milli-scale continuous reaction systems a detailed understanding of multiphase flow systems and the underlying physics of the transport processes is needed. In this paper, we investigate interfacial mass transfer in liquid–liquid flow of water and 1-butanol on the micro- and the milli-scale by comparing microreactor results with two Corning reactors. Furthermore, we address the scalability of the involved mass transfer coefficients and their correlation to the observed two-phase flow pattern in the individual reactors.

The results obtained in this study quantify the influence of the flow pattern on interfacial mass transfer for two-phase flow of immiscible liquids with low interfacial tension. Furthermore, they show the importance of fluid–structure interaction on the milli-scale to equal the mass transfer performance of micro-systems and to provide predictable scale-up.

## 2. Experimental methods

### 2.1. Flow description

As a test system to quantify interfacial mass transfer we employed the extraction of succinic acid (Fluka, 99.5%) from the organic phase (1-butanol, Sigma-Aldrich, anhydrous 99.8%) with an aqueous phase (deionized water). The system 1-butanol/succinic acid/water is a standard test system with low interfacial surface tension recommended by the European Federation of Chemical Engineering (Misek et al., 1985). The physical properties of the components are summarized in Table 1.

The scale-up of the mass transfer coefficient was investigated over three different length scales using a standard microreactor with spiral design and two Corning reactors, namely the Low-Flow Reactor (LFR), and the Advanced-Flow Reactor (AFR), which are depicted in Fig. 1. The microreactor (Fig. 1 left) features a small meandering mixing section which is followed by a spiral channel.

**Table 1**
Physical properties of the fluids used for the mass transfer study (Misek et al., 1985).

| Property | Fluid | |
|---|---|---|
| | Water | 1-butanol |
| Density $\varrho$ (kg/m$^3$) | 998 | 810 |
| Viscosity $\eta$ (Pa s) | 1.00e−3 | 2.95e−3 |
| Interfacial tension $\sigma$ (N/m) | 8.00e−4 | |

The liquids entered into the reactor using the first two inlets, the third was inactive for the present study. These devices were fabricated from a double-polished silicon wafer and a Pyrex wafer (diameter, 150 mm; thickness, 650 μm). The fabrication process consisted of several photolithography steps, deep reactive-ion etching of silicon, and the growth of silicon nitride (0.5 μm) (Jensen, 2006; Bedore et al., 2010). The microreactors were connected to inlet and outlet fluid tubes by mounting them on a compression stainless steel device (Zaborenko et al., 2011). At the outlet the two phase system was separated by settling and the water phase was immediately transferred to a separate glass container. The aqueous phase was subsequently analyzed by titration with a 0.1 M NaOH solution (Fluka, volumetric standard). In the case of the microreactor the liquids were delivered by syringe pumps (Harvard Apparatus HP 2000). In addition to the standard silicone nitride reactor we also used a Teflon coated reactor (Kuhn et al., 2011) to investigate the influence of surface wettability on mass transfer in liquid–liquid flows.

In the Corning flow reactors, the two fluids first make contact by means of a nozzle. The mixing part of the reactor is composed of single heart shaped elements. In these sections the fluid is mixed by splitting and recombining, together with the change of flow direction induced by a solid U-shaped structure. The two split fluid streams are subsequently combined in a larger sized volume with a cylindrical glass part after the U-structure in case of the AFR (see Fig. 1 (bottom)). In the LFR design these two separate structures (the cylinder and the U-shape) are combined to a single Y-shaped glass structure which the fluid needs to bypass (see Fig. 1 (top right)). The total number of hearts in the AFR design is 51, with an overall width of 1 cm and a nozzle size of 1 mm, whereas in the LFR the total number of hearts is 32, with an overall width of 8.5 mm and a nozzle size of 0.6 mm. For both reactor types the heart shaped mixing zone is followed by a zone with straight channels before reaching the outlet. As for the microreactor, the two phase system was separated by fast settling and immediately transferring the aqueous phase to a glass container, and the aqueous phase is subsequently analyzed using titration. The reactors were fed by a single piston syringe pump, which produces a steady flow without pulsation (TELEDYNE ISCO pump, Model 260D). The channel height and the internal volume of the three reactor types used in this study are summarized in Table 2. The experiments were performed in a residence time range between 1 s and 30 s, with equal volumetric flow rates of the 1-butanol and water phase. This results in a flow rate range of 0.16–6.5 ml/min for the microreactors (two phase Reynolds number from 5.3 to 201), 0.45–10.3 ml/min for the Corning LFR (two phase Reynolds number from 17.2 to 393), and 8.7–200.0 ml/min for the Corning AFR (two phase Reynolds number from 146.0 to 3357).

### 2.2. Mass transfer quantification

Using succinic acid as the mass transfer component enables the following extraction process by monitoring the change of pH of the aqueous phase, and the volumetric mass transfer coefficient $k_La$ is determined from the titration results. By applying a mass balance over the entire reactor, the equation to calculate $k_La$ reads (Yue et al., 2007)

$$k_La = \frac{1}{\tau}\ln\left(\frac{C^*_{aq} - C_{aq,i}}{C^*_{aq} - C_{aq,o}}\right) \quad (1)$$

where $k_L$ is the overall mass transfer coefficient, $a$ is the specific interfacial area, and $\tau$ denotes the residence time which is calculated from the flow rates of the phases $\dot{V}_i$ ($i$ equals $aq$ and $org$ for the aqueous and organic phases, respectively), and the reactor

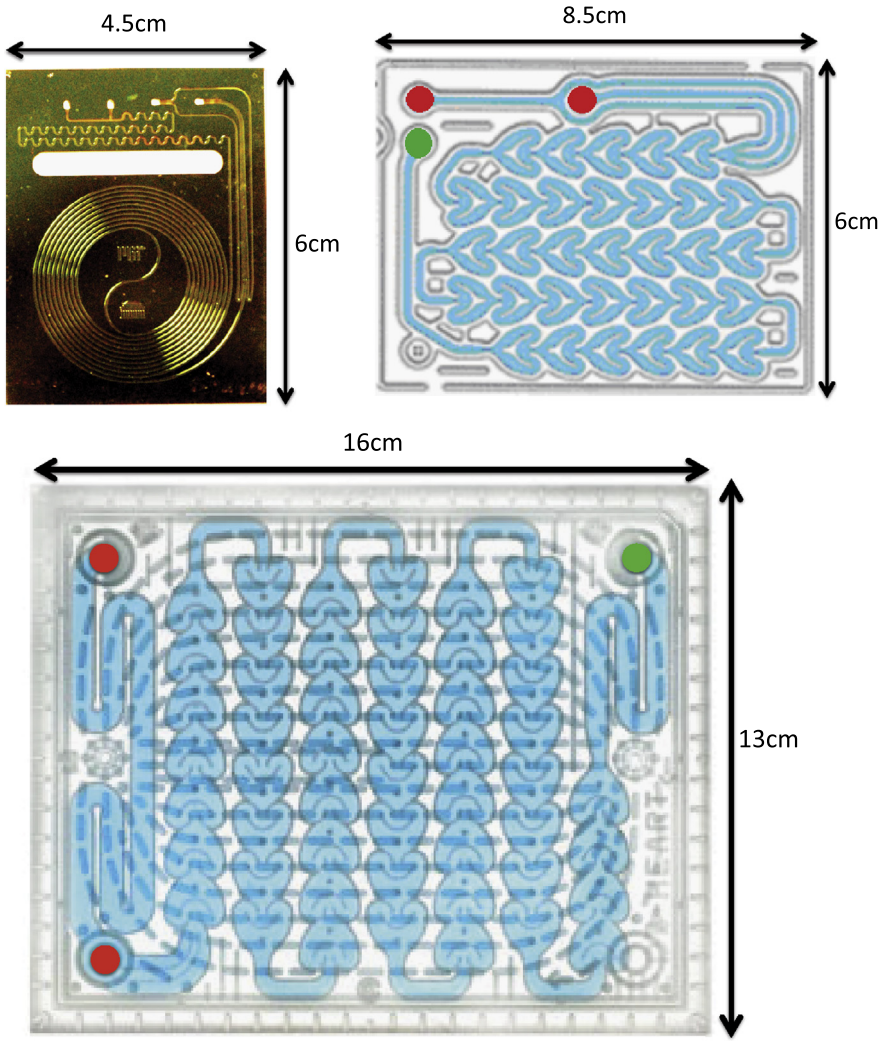


**Fig. 1.** Schematic representations of the microreactor (top left), the Corning LFR (top right), and the Corning AFR (bottom) [not to scale].

**Table 2**
Dimensions of the used micro- and Corning reactors.

| Reactor type | Channel height (m) | Volume $V_R$ ($m^3$) |
|---|---|---|
| Spiral microreactor (nitride) | $4.27 \times 10^{-4}$ | $1.60 \times 10^{-7}$ |
| Spiral microreactor (Teflon) | $5.00 \times 10^{-4}$ | $2.27 \times 10^{-7}$ |
| Corning LFR | $4.00 \times 10^{-4}$ | $4.50 \times 10^{-7}$ |
| Corning AFR | $1.10 \times 10^{-3}$ | $8.70 \times 10^{-6}$ |

volume $V_R$:

$$\tau = \frac{V_R}{\dot{V}_{aq} + \dot{V}_{org}} \tag{2}$$

$C_{aq,i}$ is the concentration of the transfer component in the water phase at the inlet (which is zero for our experimental conditions) and $C_{aq,o}$ at the outlet. $C^*_{aq}$ denotes the equilibrium concentration of the transfer component in the aqueous phase which is defined by the partition coefficient between the two-phases, and was determined experimentally for each run by stirring the starting solutions overnight and subsequent titration of the aqueous phase.

To quantify the overall extraction in a given reactor, we additionally calculate the extraction efficiency $E$ which describes the concentration difference reached between the channel inlet and outlet compared to the maximal possible concentration difference defined by the difference between the inlet concentration and the equilibrium between the phases:

$$E = \frac{(C_{aq,i} - C_{aq,o})}{(C_{aq,i} - C^*_{aq})} \tag{3}$$

## 3. Results

In a first step, we quantify liquid–liquid mass transfer in the hydrophilic silicon nitride and the hydrophobic Teflon coated microreactors with spiral design. The overall mass transfer coefficient $k_La$ subject to the residence time is depicted in Fig. 2 (top). No influence of surface wettability is observed as both reactors exhibit similar mass transfer characteristics, however, a sharp increase for residence times below $\tau = 3$ s is found. This behavior is also seen in Fig. 2 (bottom), which depicts the extraction efficiency $E$. Three different regimes can be identified: (i) for residence times above 10 s the extraction is nearly complete, i.e. the concentration at the outlet of the reactor is close to the equilibrium concentration; (ii) for the residence time range between 3 s and 10 s a steady decrease in the extraction efficiency is observed; and (iii) for residence times below 3 s the extraction efficiency is again increasing. These findings suggest a transition in the mass transfer mechanism linked to the two-phase flow pattern in the microreactor. Thus we applied laser-induced fluorescence (LIF) by adding Rhodamine 6G to the water phase to capture the

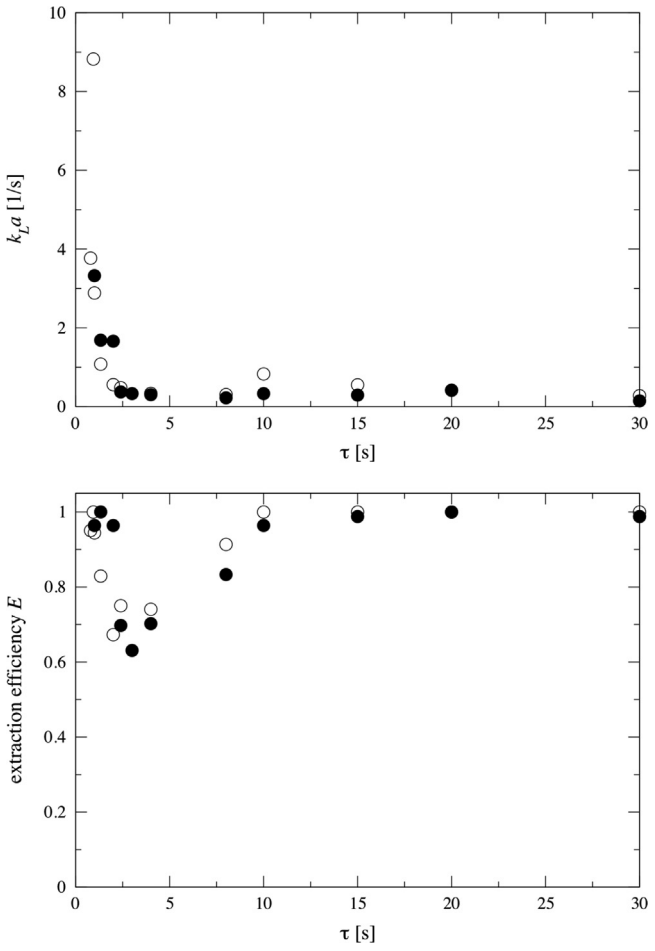


**Fig. 2.** Volumetric mass transfer coefficient $k_{La}$ (top) and extraction efficiency $E$ (bottom) for microreactors with a nitride (○) and Teflon (•) coating.

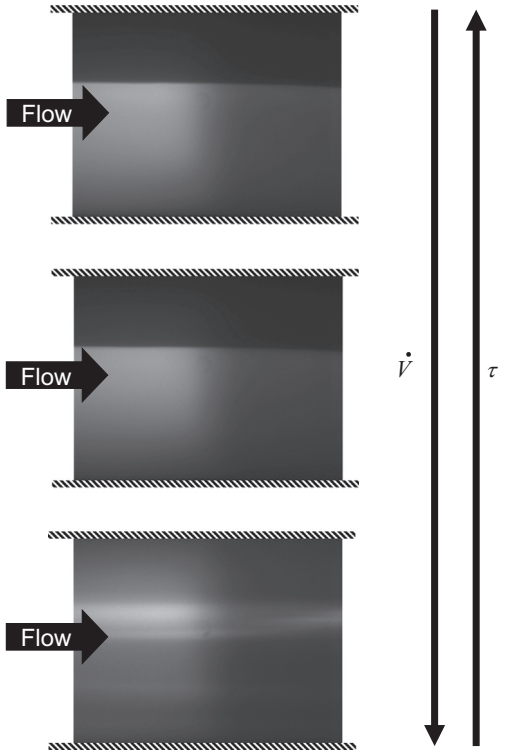


**Fig. 3.** Microscope images of the nitride coated microreactor with decreasing $\tau$ (top to bottom: $\tau$=30 s, 20 s, 1 s). The bright colored phase represents water, the dark colored phase represents 1-butanol. (For interpretation of the references to color in this figure caption, the reader is referred to the web version of this paper.)

phase distribution and the prevailing flow pattern (e.g. Crimaldi, 2008; Wagner et al., 2007; Kuhn and Jensen, 2012). The LIF measurements were performed using an inverted fluorescence microscope (Zeiss Axiovert 200). We used a 10× microscope objective with a numerical aperture of 0.30, which resulted in a field of view (FOV) of $0.76 \times 0.58$ mm$^2$. Furthermore, the microscope was equipped with a 605/70 nm bandpass filter for the emitted light. The light source was provided by a frequency-doubled Nd:YAG laser (BigSky Ultra CFR, 30 mJ, 532 nm) coupled to the microscope using a dichroic mirror. The images were recorded using a dual-frame CCD camera (PCO Sensicam QE, $1376 \times 1024$ pixels$^2$, 8bit). Fig. 3 depicts microscope images of the nitride coated microreactor subject to the residence time, where the bright colored phase represents water and the dark colored phase represents 1-butanol. Stratified flow is observed for residence times of 20 s and 30 s, where two separate layers of 1-butanol and water flow side by side with a different velocity relative to each other. Due to their difference in viscosity, the 1-butanol phase occupies a smaller channel cross-section and consequently flows with a higher local velocity than the water phase, while keeping the inlet flow rates of both phases identical through the syringe pumps. By further deceasing the residence time below $\tau$=3 s the stratification is vanishing and the two-phase flow is dispersed (as shown for $\tau$=1 s in Fig. 3(bottom)). Due to the low interfacial tension two-phase Taylor flow is only observed for residence times above 60 s. These two-phase flow patterns explain the observed regimes in mass transfer and extraction efficiency. In stratified flow the interfacial area $a$ is constant and independent of the flow rates, thus the extraction efficiency is only governed by the contact time of the two phases, which corresponds to the residence time. This leads to the decrease in extraction efficiency observed for residence times below 10 s. However, below $\tau$=3 s the two-phase flow starts to disperse, and thus to significantly increase the interfacial area and the mass transfer. These findings also explain that the microchannel wettability has no influence on the extraction resulting in these range of residence times, as there is no dispersed or continuous phase. In a previous study concerned with the synthesis of nanomaterials in two-phase flow (Sebastian Cabeza et al., 2012) an effect of the wall wettability on the nanoparticle size distribution was found. This result is explained by the fact that changing the wall properties influences the internal mixing in the liquid slug, which in turn will also affect the interfacial mass transfer. However, it is important to note that during the nanoparticle synthesis the microreactors were operating in a different flow regime, namely segmented flow (Taylor flow), whereas the present study is concerned with stratified and dispersed flow. And in this flow pattern a change in the wall wettability will not affect the mass transfer as the active interfacial area is located close to the center of the channel, and thus not influenced by the wall properties.

In the next step we advance to the Corning flow reactors, and the overall mass transfer coefficient $k_L a$ subject to the residence time is depicted in Fig. 4 (top). As for the microreactors, the graphs for the Corning reactors show an inverse dependency of the mass transfer coefficient on $\tau$. Furthermore, there is no significant difference between the two studied types of reactors, despite their different dimensions (i.e. channel height and nozzle width) and layouts (i.e. number of hearts and shape of the solid obstacles). When advancing from the LFR to the AFR the resulting reactor volume is increased by one order of magnitude, but still nearly identical values of the overall mass transfer coefficient $k_L a$ are observed. This clearly shows the potential in using the Corning

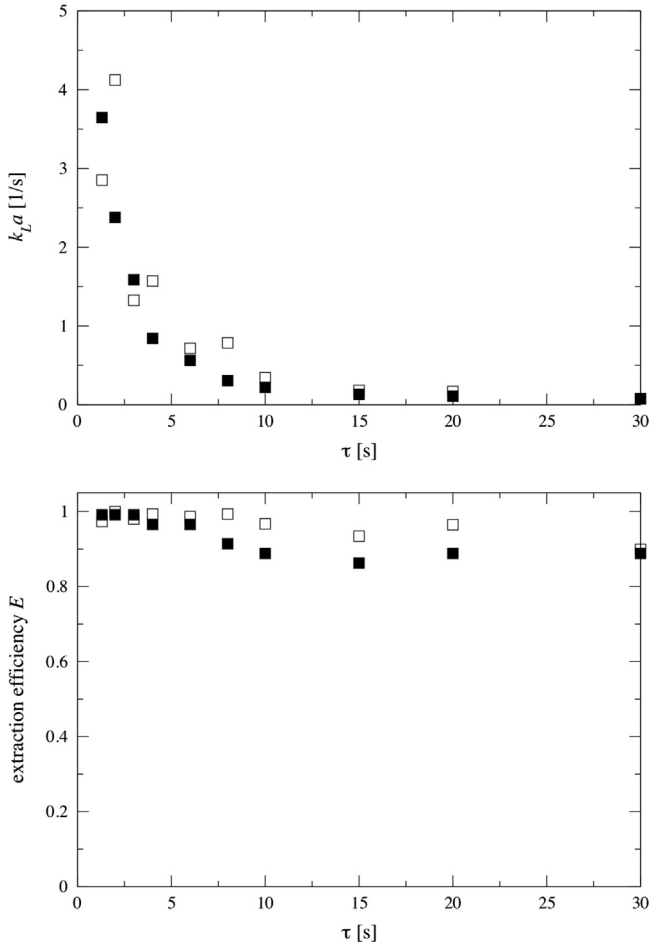


**Fig. 4.** Volumetric mass transfer coefficient $k_L a$ (top) and extraction efficiency $E$ (bottom) for the Corning LFR (■) and AFR (□).

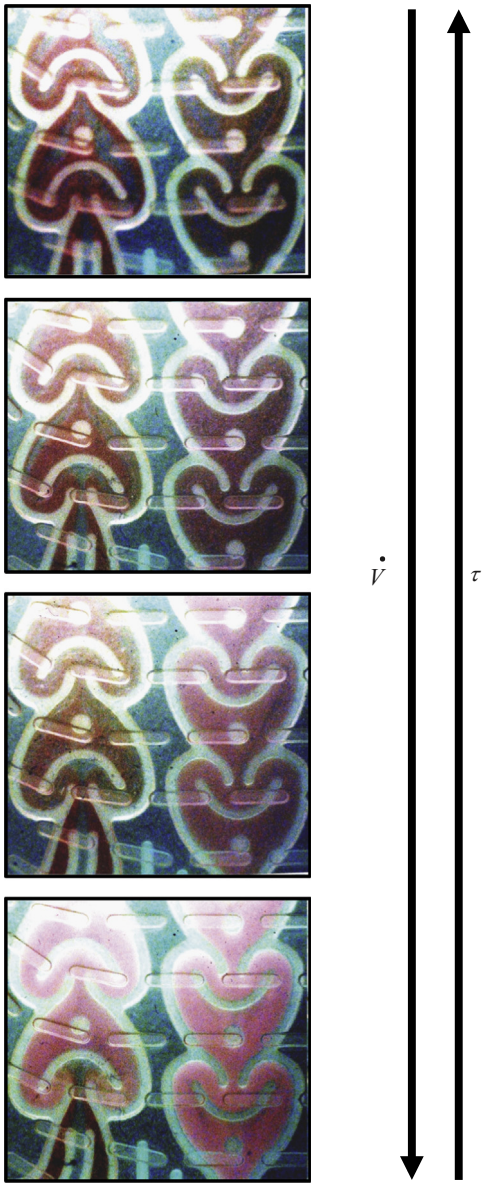


**Fig. 5.** Photographs of the Corning AFR with decreasing $\tau$ (top to bottom: $\tau$=30 s, 10 s, 5 s, 1 s). The red colored phase represents water, the blue colored phase represents 1-butanol. (For interpretation of the references to color in this figure caption, the reader is referred to the web version of this paper.)

flow reactors for flow chemistry applications, as this similarity in mass transfer coefficients facilitates the scale-up for reaction mixtures involving immiscible fluids.

The extraction efficiency $E$ is plotted in Fig. 4 (bottom), and increasing values are observed with increasing flow rate (decreasing residence time). Contrary to the microreactors, the extraction does not reach equilibrium for the highest residence times investigated, but the sudden drop in extraction efficiency in the intermediate residence time range is also not observed, only a slight decrease is apparent for the LFR configuration. Below $\tau$=3 s the extraction process is nearing completion, i.e. the extraction efficiency is approaching its limit of $E \approx 1$. This increase in extraction efficiency despite the decreasing contact time indicates that the two-phase mixing is steadily improved with increasing flow rate.

To illustrate this effect, we again applied Rhodamine 6G to the water phase and took high-resolution photographs using a still camera (Nikon D200). Fig. 5 shows the phase distribution in the Corning AFR subject to residence time, where the red colored phase represents water and the blue colored phase represents 1-butanol. Each image shows the first 2 hearts of the first row of the reactor, and the last 2 hearts in the second row. For the highest residence time investigated the two-phase flow is stratified, and even in the second row the water and 1-butanol phases are clearly distinguishable and flowing parallel, thus the phase dispersion is identical to the inlet region. When further increasing the flow rate, the separate flows start getting interrupted, which further enhances the mixing and enlarges the interfacial area between the two phases. For these flow rates the 1-butanol flow and the water flow do no longer flow side by side, but they intrude into each other. As a result, the mixing quality is enhanced after flowing through several hearts. For the second highest flow rate, the mixing in the second row is so far developed that no phase separation can be observed. For the highest flow rate the phases are already indistinguishable in the first heart. Generally, it is observed that an increasing flow rate improves the phase dispersion and as a consequence the extraction efficiency is steadily improved.

For a concise comparison across the device scales, Fig. 6 depicts the volumetric mass transfer coefficient $k_L a$ (top) and the extraction efficiency $E$ (bottom) for the microreactors and the Corning systems. It is remarkable that especially for the mass transfer coefficient the order of magnitude at a given residence time is similar across all investigated reactor types. For $\tau > 10$ s a slightly higher $k_L a$ value is observed for the microreactors, at these flow rates the flow is stratified in all devices, but the microreactors

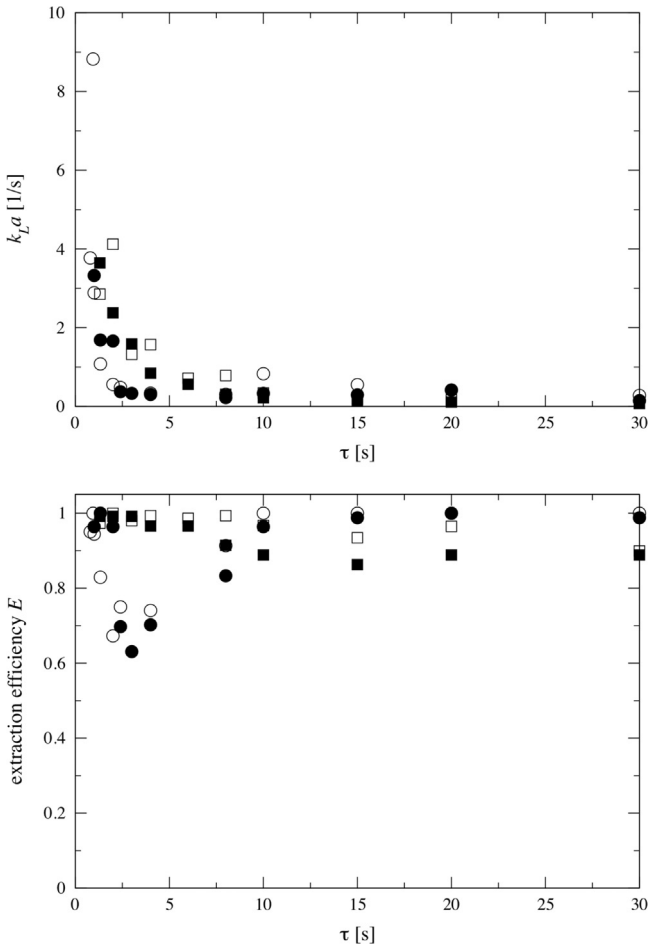


**Fig. 6.** Volumetric mass transfer coefficient $k_La$ (top) and extraction efficiency $E$ (bottom) for microreactors with a nitride (○) and Teflon (●) coating, and the Corning LFR (■) and AFR (□).

provide an increased surface-to-volume ratio which is beneficial to the extraction process in this regime. In the range 3 s $< \tau <$ 10 s the Corning systems perform slightly better, as their particular design induces fluid–structure interactions which steadily improve the phase dispersion and hence the interfacial area and mass transfer. This is contrary to the microreactors, where stratified flow is still observed in this residence time range and the contact time between the phases is no longer sufficient to complete the extraction process. For $\tau < 3$ s the micro- and millireactors perform similarly.

In Table 3 the liquid–liquid mass transfer coefficients obtained in this work are compared to available literature studies. Di Miceli Raimondi et al. (2014) investigated the liquid–liquid mass transfer using the test system water and toluene, with acetone as the mass transfer component, in square microchannels of 210 μm, and 300 μm respectively. The obtained volumetric mass transfer coefficients range from 0.72 to 8.44 $s^{-1}$ for droplet velocities of 0.02–0.35 m/s, and for the entire range of residence times slug flow was observed. This might also explain the slightly higher $k_La$ values measured by Di Miceli Raimondi et al. (2014) in comparison to the microreactors addressed in the present work. In contrast to the stratified flow regime, secondary flow structures are present in slug flow which further improve the interfacial mass transfer and mixing (e.g. Günther et al., 2005; Kuhn and Jensen, 2012). But it is also worth mentioning that the reported $k_La$ values are nevertheless in the same order of magnitude compared to all flow reactors investigated in the present work. In the work of Assmann and Rudolf Von Rohr (2011) elevated values for the liquid–liquid mass transfer coefficient are reported, however this is determined by the low range of residence times (below 1 s for all experimental conditions) and the addition of an inert gas to form a gas–liquid–liquid flow. After establishing this flow regime, an alternating pattern of gas bubbles and dispersed droplets in the continuous liquid phase is formed, which additionally increases secondary flow motions and enhances interfacial mass transfer. In a comprehensive study, Kashid et al. (2011) investigated the influence of the channel cross-sectional shape on liquid–liquid mass transfer. For this microchannels of square, trapezoidal and rectangular cross-sections were compared, and the largest $k_La$ value is observed for the square geometry, followed by the trapezoidal and the rectangular cross-section. Thus interfacial mass transfer is influenced by the two-phase contacting geometry, which can be explained by changes in the liquid film thickness in the corners of the channel (Fries et al., 2008). Ghaini et al. (2010) and Kashid et al. (2007) investigated liquid–liquid slug flow in capillary microreactors with internal diameters ranging from 500 μm to 1 mm. In both works, a decrease in the mass transfer coefficient when increasing the capillary diameter is observed, which indicates a decrease in mass transfer performance when scaling-up. However, this is not reflected in the results of the present study, where similar $k_La$ values are found across all flow reactor systems and length scales, which further highlights the mass transfer efficient design of the Corning reactors. Dessimoz et al. (2008) observed similar mass transfer coefficients for slug flow and stratified flow. However, it has to be noted that these studies have been performed in microchannels with different inlet geometries (Y- and T-junction), which are known to affect the two-phase flow formation (e.g. van Steijn et al., 2007; Abate et al., 2009) and might have impacted the observed mass transfer coefficients as well.

## 4. Conclusions

Interfacial mass transfer in liquid–liquid flow was addressed by investigating the extraction of succinic acid from 1-butanol with water. The low interfacial tension between water and 1-butanol results in stratified or dispersed two-phase flow, Taylor flow was only observed in residence time ranges outside the scope of this study. The scale-up of the mass transfer coefficient was investigated over three different length scales using standard microreactors and two Corning reactors.

For all systems it was found that the increase in observed overall mass transfer and extraction efficiency is directly linked to the transition from stratified to dispersed flow. In the stratified regime higher $k_La$ and $E$ values are observed for the microreactor systems, which is explained by the advantages associated with the small length-scale, i.e. the increased surface-to-volume ratio. For very low residence times, which results in the two-phase flow being in the fully dispersed regime, an equal mass transfer performance between the devices is observed. The results of the intermediate residence time regime highlight the importance of the particular design of the milli-scale systems. The heart shape and the presence of obstacles enhance fluid–structure interactions, which in turn lead to increased mixing and phase dispersion. These interactions provide the necessary energy to interrupt the flow stratification and to increase the interfacial area (which enhances the extraction efficiency and the mass transfer coefficient). On the micro-scale, the interruption of the flow stratification can only be achieved by increasing the flow rates, i.e. increasing the shear between the phases is the only available energy source for flow regime transition. As a result, the Corning systems exhibit a steady increase in extraction efficiency and mass

**Table 3**
Comparison of liquid–liquid mass transfer coefficients in micro- and milli-scale reactors.

| Geometry | $k_La$ ($s^{-1}$) | Reference |
|---|---|---|
| Microreactor (Nitride), 427 μm | 0.28–8.83 | Present work |
| Microreactor (Teflon), 500 μm | 0.15–3.33 | Present work |
| Corning LFR, 400 μm | 0.07–3.65 | Present work |
| Corning AFR, 1.1 mm | 0.07–3.31 | Present work |
| Microchannel, 210 μm | 1.61–8.44 | Di Miceli Raimondi et al. (2014) |
| Microchannel, 300 μm | 0.72–2.65 | Di Miceli Raimondi et al. (2014) |
| Microchannel, 220 μm | 5.00–12.0 | Assmann and Rudolf Von Rohr (2011) |
| Square microchannel, 400 μm | 0.11–0.74 | Kashid et al. (2011) |
| Trapezoidal microchannel, 400 μm | 0.16–0.44 | Kashid et al. (2011) |
| Rectangular microchannel, 269 μm | 0.05–0.20 | Kashid et al. (2011) |
| Concentric capillary, 1.6 mm | 0.01–0.06 | Kashid et al. (2011) |
| Caterpillar (IMM), 150 μm | 0.12–0.68 | Kashid et al. (2011) |
| Capillary, 500 μm | 0.90–1.67 | Ghaini et al. (2010) |
| Capillary, 750 μm | 0.91–1.46 | Ghaini et al. (2010) |
| Capillary, 1 mm | 0.88–1.29 | Ghaini et al. (2010) |
| Microchannel, 400 μm | 0.20–0.50 | Dessimoz et al. (2008) |
| Capillary, 500 μm | 0.12–0.31 | Kashid et al. (2007) |
| Capillary, 750 μm | 0.07–0.15 | Kashid et al. (2007) |
| Capillary, 1 mm | 0.02–0.09 | Kashid et al. (2007) |
| Microchannel, 380 μm | ≈0.50 | Burns and Ramshaw (2001) |

transfer coefficient, whereas on the micro-scale a step change with the sudden flow regime transition is observed.

This study also highlighted that using this particular heart shape design of the Corning Advanced Flow Reactors leads to the direct scalability of the mass transfer coefficients from the micro- to the milli-scale. This observation underpins the feasibility of using these reactors in the screening and development phases for continuous flow reactions.

The results obtained in this study quantify the influence of the flow pattern on interfacial mass transfer for two-phase flow of immiscible liquids with low interfacial tension. Furthermore, they show the importance of fluid–structure interaction on the milli-scale to equal the mass transfer performance of micro-systems and to provide predictable scale-up.

## Notation

*Roman symbols*

| | |
|---|---|
| $a$ | interfacial area ($m^2\ m^{-3}$) |
| $C_i$ | species concentration (mole $m^{-3}$) |
| $C^*$ | equilibrium concentration (mole $m^{-3}$) |
| $D$ | diameter (m) |
| $E$ | extraction efficiency (–) |
| $k_L$ | liquid side mass transfer coefficient ($m\ s^{-1}$) |
| $V_R$ | reactor volume ($m^3$) |
| $\dot{V}_i$ | flow rate ($m^3\ s^{-1}$) |

*Greek symbols*

| | |
|---|---|
| $\varrho$ | density ($kg\ m^{-3}$) |
| $\eta$ | dynamic viscosity (Pa s) |
| $\sigma$ | interfacial tension ($N\ m^{-1}$) |
| $\tau$ | residence time (s) |

*Abbreviations*

| | |
|---|---|
| AFR | Advanced-Flow Reactor |
| LFR | Low-Flow Reactor |

## Acknowledgments

This work has been funded by the Novartis-MIT Center for Continuous Manufacturing, and we appreciate Corning for donating their AFR and LFR systems for these studies. A.W. was a visiting student from Technische Universität München, and acknowledges financial support from the Ernest-Solvay-Foundation, S.K. acknowledges funding from the Swiss National Science Foundation (SNF).

## References

Abate, A., Poitzsch, A., Hwang, Y., Lee, J., Czerwinska, J., Weitz, D., 2009. Impact of inlet channel geometry on microfluidic drop formation. Phys. Rev. E 80, 026310.
Anderson, N., 2012. Using continuous processes to increase production. Org. Process Res. Dev. 16, 852–869.
Assmann, N., Rudolf Von Rohr, P., 2011. Extraction in microreactors: intensification by adding an inert gas phase. Chem. Eng. Process.: Process Intensif. 50, 822–827.
Bedore, M.W., Zaborenko, N., Jensen, K.F., Jamison, T.F., 2010. Aminolysis of epoxides in a microreactor system: a continuous flow approach to $\beta$-amino alcohols. Org. Process Res. Dev. 14, 432–440.
Burns, J.R., Ramshaw, C., 2001. The intensification of rapid reactions in multiphase systems using slug flow in capillaries. Lab Chip 1, 10–15.
Crimaldi, J.P., 2008. Planar laser induced fluorescence in aqueous flows. Exp. Fluids 44, 851–863.
Dessimoz, A.L., Cavin, L., Renken, A., Kiwi-Minsker, L., 2008. Liquid–liquid two-phase flow patterns and mass transfer characteristics in rectangular glass microreactors. Chem. Eng. Sci. 63, 4035–4044.
Di Miceli Raimondi, N., Prat, L., Gourdon, C., Tasselli, J., 2014. Experiments of mass transfer with liquid–liquid slug flow in square microchannels. Chem. Eng. Sci. 105, 169–178.
Ehrfeld, W., Hessel, V., Loewe, H., 2000. Microreactors: New Technology for Modern Chemistry. Wiley-VCH, Weinheim, Germany.
Fries, D.M., Trachsel, F., von Rohr, P.R., Rudolf von Rohr, P., 2008. Segmented gas–liquid flow characterization in rectangular microchannels. Int. J. Multiph. Flow 34, 1108–1118.
Ghaini, A., Kashid, M., Agar, D., 2010. Effective interfacial area for mass transfer in the liquid–liquid slug flow capillary microreactors. Chem. Eng. Process.: Process Intensif. 49, 358–366.
Günther, A., Jhunjhunwala, M., Thalmann, M., Schmidt, M.A., Jensen, K.F., 2005. Micromixing of miscible liquids in segmented gas–liquid flow. Langmuir 21, 1547–1555.
Hartman, R.L., Naber, J.R., Buchwald, S.L., Jensen, K.F., 2010. Multistep microchemical synthesis enabled by microfluidic distillation. Angew. Chem. 49, 899–903.
Hessel, V., Noël, T., 2012a. Micro process technology, 1. Introduction. In: Ullmann's Encyclopedia of Industrial Chemistry.
Hessel, V., Noël, T., 2012b. Micro process technology, 2. Processing. In: Ullmann's Encyclopedia of Industrial Chemistry.
Hessel, V., Wang, Q., 2011. Novel process windows. Part 1: boosted micro process technology. Chim. Oggi (Chem. Today) 29.
Jensen, K.F., 2001. Microreaction engineering—is small better? Chem. Eng. Sci. 56, 293–303.
Jensen, K.F., 2006. Silicon-based microchemical systems: characteristics and applications. MRS Bull. 31, 101–107.
Jimenez-Gonzalez, C., Poechlauer, P., Broxterman, Q., Yang, B., am Ende, D., Baird, J., Bertsch, C., Hannah, R., Dell'Orco, P., Noorman, H., Yee, S., Reintjens, R., Wells, A., Massonneau, V., Manley, J., 2011. Key green engineering research areas for sustainable manufacturing: a perspective from pharmaceutical and fine chemicals manufacturers. Org. Process Res. Dev. 15, 900–911.

Kashid, M.N., Harshe, Y.M., Agar, D.W., 2007. Liquid–liquid slug flow in a capillary: an alternative to suspended drop or film contactors. Ind. Eng. Chem. Res. 46, 8420–8430.
Kashid, M.N., Renken, A., Kiwi-Minsker, L., 2011. Influence of flow regime on mass transfer in different types of microchannels. Ind. Eng. Chem. Res. 66, 3876–3897.
Kuhn, S., Hartman, R.L., Sultana, M., Nagy, K.D., Marre, S., Jensen, K.F., 2011. Teflon-coated silicon microreactors: impact on segmented liquid–liquid multiphase flows. Langmuir 27, 6519–6527.
Kuhn, S., Jensen, K.F., 2012. A pH sensitive laser-induced fluorescence technique to monitor mass transfer in multiphase flows in microfluidic devices. Ind. Eng. Chem. Res. 51, 8999–9006.
Lavric, E., 2008. Thermal performance of Corning glass microstructures. In: International Conference on Heat Transfer and Fluid Flow in Microscale.
McMullen, J.P., Stone, M.T., Buchwald, S.L., Jensen, K.F., 2010. An integrated microreactor system for self-optimization of a heck reaction: from micro- to mesoscale flow systems. Angew. Chem. 49, 7076–7080.
Misek, T., Berger, R., Schroter, J., 1985. Standard test systems for liquid extraction. Published on behalf of the European Federation of Chemical Engineering by Institution of Chemical Engineers.
Nieves-Remacha, M.J., Kulkarni, A.A., Jensen, K.F., 2012. Hydrodynamics of liquid–liquid dispersion in an advanced-flow reactor. Ind. Eng. Chem. Res. 51, 16251–16262.
Nieves-Remacha, M.J., Kulkarni, A.A., Jensen, K.F., 2013. Gas–liquid flow and mass transfer in an advanced flow reactor. Ind. Eng. Chem. Res. 52, 8996–9010.
Sebastian Cabeza, V., Kuhn, S., Kulkarni, A.A., Jensen, K.F., 2012. Size-controlled flow synthesis of gold nanoparticles using a segmented flow microfluidic platform. Langmuir 28, 7007–7013.
van Steijn, V., Kreutzer, M.T., Kleijn, C.R., 2007. mPIV study of the formation of segmented flow in microfluidic T-junctions. Chem. Eng. Sci. 62, 7505–7514.
Wagner, C., Kuhn, S., Rudolf von Rohr, P., 2007. Scalar transport from a point source in flows over wavy walls. Exp. Fluids 43, 261–271.
Yue, J., Chen, G., Yuan, Q., Luo, L., Gonthier, Y., 2007. Hydrodynamics and mass transfer characteristics in gas–liquid flow through a rectangular microchannel. Chem. Eng. Sci. 62, 2096–2108.
Zaborenko, N., Bedore, M., Jamison, T.F., Jensen, K.F., 2011. Kinetic and scale-up investigations of epoxide aminolysis in microreactors at high temperatures and pressures. Org. Process Res. Dev. 15, 131–139.
Zhang, F., Cerato-Noyerie, C., Woehl, P., Lavric, E., 2011. Intensified liquid–liquid mass transfer in corning advanced-flow reactors. Chem. Eng. Trans. 24, 1369–1374.